



# The role of geomorphology, rainfall and soil moisture in the occurrence of landslides triggered by 2018 Typhoon Mangkhut in the Philippines

Clàudia Abancó<sup>1</sup>, Georgina L. Bennett<sup>1</sup>, Adrian J. Matthews<sup>2</sup>, Mark A. Matera<sup>3</sup>, Fabor J. Tan<sup>3</sup>

5 <sup>1</sup>College of Life and Environmental Sciences, University of Exeter, Exeter, EX4 4RJ, United Kingdom

<sup>2</sup>Centre for Ocean and Atmospheric Sciences, School of Environmental Sciences and School of Mathematics, University of East Anglia, Norwich, NR4 7TJ, United Kingdom

<sup>3</sup>School of Civil, Environmental and Geological Engineering, Mapua University, Manila, Philippines

10 *Correspondence to:* Clàudia Abancó (c.abanco@exeter.ac.uk)

## Abstract

*In 2018, Typhoon Mangkhut (locally known as Typhoon Ompong) triggered thousands of landslides in the area of Itogon (Philippines). A landslide inventory of 1101 landslides over a 570 km<sup>2</sup> area is used to study the geomorphological characteristics and land cover more prone to landsliding as well as the rainfall and soil moisture conditions that led to widespread failure. Landslides mostly occurred in slopes covered by wooded grassland in clayey materials, predominantly facing East-Southeast. The analysis of both satellite rainfall (GPM IMERG) and soil moisture (SMAP-L4) finds that, in addition to rainfall from the typhoon, soil water content plays an important role in the triggering mechanism. Rainfall associated with Typhoon Mangkhut is compared with 33 high intensity rainfall events that did not trigger regional landslide events in 2018 and with previously published rainfall thresholds. Results show that: a) it was one of the most intense rainfall events in the year but not the highest, and b) despite satellite data tending to underestimate intense rainfall, previous published regional and global thresholds are to be too low to discriminate between landslide triggering and non-triggering rainfall events. This work highlights the potential of satellite products for hazard assessment and early warning in areas of high landslide activity where ground-based data is scarce.*

15  
20

## 1 Introduction

25 Landslides driven by typhoon and monsoon rainfall cause thousands of fatalities and millions of pesos in damage to infrastructure and commerce in the Philippines each year. The Philippines accounts for 46% of rainfall-triggered landslides in SE Asia, although it represents only 6% of the land area (Kirschbaum et al., 2015; Petley, 2012). The climate characteristics, with frequent tropical cyclones and two different monsoon regimes, together with abrupt orography and unstable geologic materials make the terrain prone to Multiple-Occurrence Regional Landslide Events (MORLEs) (Crozier, 2005). Despite the  
30 relevance of the phenomena, the understanding of the triggering conditions and the instability mechanisms associated with



rainfall triggered MORLEs in the Philippines has still received little attention. This, combined with the incomplete landslide records and the shortage of landslide inventories, results in hazard and risk assessment techniques that still lack accuracy in the country.

35 The understanding of MORLEs and the assessment of their impact relies on the availability of landslide inventories (Crozier, 2005; Martino et al., 2020; Shu et al., 2019). Landslide inventories are key to evaluate the probability of slope failure, based on the conditions of previous slope failures and the effects of local terrain conditions across a region as a preliminary step toward landslide susceptibility, hazard and risk assessment (Fell et al., 2008; Guzzetti et al., 2005, 2012). Regardless of their importance, landslide inventories are often not available due to incomplete event records, or as a result of the lack of time and  
40 resources to update them, for example in response to extreme events (Malamud et al., 2004). To map landslides across large regions using manual techniques is a highly time consuming task, and although the use of automatic mapping tools is increasing (Alvioli et al., 2018; Borghuis et al., 2007; Kirschbaum and Stanley, 2018; Scheip and Wegmann, 2020), their widespread applicability still presents some limitations. It is particularly challenging in regions hit by the passage of typhoons, where the area affected by landslides can be up to hundreds of km<sup>2</sup> (e.g.: Tseng et al., 2015).

45 In the Philippines, a nationwide inventory of >12000 landslides is available (Lagmay et al., 2017). However, most of the landslides are mapped as points rather than polygons, precluding magnitude-frequency analysis, a major component of landslide hazard assessment (Guzzetti et al., 2005). The use of polygon landslide inventories instead allows the retrieval of the landslide magnitude distribution (e.g.: Malamud et al., 2004; Parker et al., 2011). A limited number of studies including the  
50 analysis of landslide conditioning factors in the area of Baguio have been published (Nolasco-Javier et al., 2015; Nolasco-Javier and Kumar, 2019), however the Philippines lacks a more detailed landslide susceptibility studies that may help in local planning. For example, the Philippines' Mines and Geosciences Bureau (MGB) hazard map for the area of Itogon (Benguet, Luzon) is based on extreme scenario and hence, classes most of the region at the highest hazard level, making land use planning difficult.

55 The analysis of the triggering rainfall conditions is also fundamental to understand MORLEs. The study of landslide triggering rainfalls has been of interest of the scientific community in recent decades, generating extensive literature. One of the most common approaches for the prediction of landslide triggering rainfalls is the definition of rainfall thresholds. Rainfall thresholds are used to characterise the rainfall conditions that, when reached or exceeded are likely to trigger one or more  
60 landslides or torrential flows (De Vita et al., 1998). Different state of the art techniques and methodologies to obtain rainfall thresholds are reviewed by Segoni et al. (2018), while their applications for early warning purposes are assessed by Guzzetti et al. (2020). Two main approaches are used to derive such thresholds: a) physically-based models, where infiltration and hydrologic behaviour of the rainfall over a susceptible soil layer is simulated (e.g.: Crosta and Dal Negro, 2003; Godt et al., 2008; Papa et al., 2013); or b) empirically derived thresholds, based on the analysis of a database of rainfalls using, for example,



65 statistical techniques (e.g.: Brunetti et al., 2010; Guzzetti et al., 2007). The thresholds are generally expressed as a correlation  
between the peak intensity of the rainfall for different durations or the relationship between the total rainfall versus its duration  
(usually in the form  $I=\alpha D^\beta$ ), although some authors also include other triggering or antecedent rainfall parameters, as  
extensively reported by Segoni et al. (2018). Aspects such as the geographical distribution, the intended use of the thresholds,  
or simply the resources available determine the source of the rainfall data used to construct thresholds. Uncertainties on the  
70 source and resolution of the data as well as on the methods used to define the rainfall events or the rainfall thresholds will be  
key to their accuracy (Abancó et al., 2016; Leonarduzzi and Molnar, 2020; Nikolopoulos et al., 2015). Rainfall thresholds are  
used with early warning purposes in several countries and regions all over the world, although not in the Philippines so far  
(Guzzetti et al., 2020).

75 The use of satellite rainfall data for forecasting landslides is still minimal compared to other rainfall data sources, such as rain  
gauges or weather radar. Rainfall estimates from satellite products tend to underestimate the rainfall measurements, compared  
to rain gauge measurements, especially during extreme events (Mazzoglio et al., 2019). This is because rain gauges are nearly  
point measurements (generally correspond to areas smaller than 1 m<sup>2</sup>) while satellite measurements are area averaged, for  
example over an area of 10 x 10 km for the Integrated Multi-satellite Retrievals for the Global Precipitation Measurement  
80 (GPM) Mission (IMERG). Therefore, if a rain gauge is located on the path of a particularly intense convective cell, its records  
will be significantly higher than measurements from satellite products, which will be averaged over the whole area. Despite  
these aspects, the usability of satellite products to forecast landslides has been proven, given that the thresholds are derived  
using the same source of satellite data (Brunetti et al., 2018). In fact, early warning systems based on satellite data are a really  
powerful tool for developing countries where rain gauges may be scarce or poorly maintained, as well as to implement early  
85 warning systems at regional scales, not just at site-based locations (Kirschbaum and Stanley, 2018; Liao et al., 2010). A clear  
advantage of the satellite rainfall products is the high spatial and temporal resolution, which enables detailed analysis of rainfall  
conditions that trigger multiple landslides over large regions.

In some regions of the world, the soil wetness at the beginning of the triggering rainfall has been proven to play a major role  
90 (Bogaard and van Asch, 2002) and therefore to help improve the early warning systems (Guzzetti et al., 2020; Krogli et al.,  
2018; Marino et al., 2020). Although in previous works in the Baguio area (Philippines) the importance of the antecedent  
rainfall has been shown to be key to understanding the triggering mechanisms of MORLEs during typhoons (Nolasco-Javier  
et al., 2015; Nolasco-Javier and Kumar, 2018), no previous work has involved the analysis of soil moisture. The Soil Moisture  
Active Passive (SMAP) satellite product is a global soil moisture dataset that has potential for analysis of landslide triggering  
95 conditions and early warning (Kirschbaum and Stanley, 2018), but as yet has not been widely used in landslide research.

The municipality of Itogon (Benguet, Luzon) and its surroundings was hit by Typhoon Mangkhut (locally known as Typhoon  
Ompong) in September 2018, which triggered thousands of landslides, including a fatal one that killed more than 80 composed



of miners and their families (Cawis, 2019). The purpose of this work was: a) to map and characterize landslides triggered by  
100 Typhoon Mangkhut for the first time, producing one of the first complete inventories for a typhoon event in the Philippines,  
b) to investigate the preconditioning and triggering rainfall and soil moisture conditions and c) examine other factors that made  
certain slopes susceptible to landslides, d) to consider the potential of satellite based rainfall and soil moisture data for early  
warning of these regional landslide events.

## 2 Study Area

### 105 2.1 Geological and geomorphological setting

Our research was conducted over an area of 570 km<sup>2</sup> at the NW of the Philippines' largest island, Luzon. The study area is  
located in the province of Benguet (16.19 to 16.31°N and 120.34 to 120.48°E), at the Southern end of the Cordillera Central  
Mountain Range, the largest mountain range of the country (Figure 1). The Eastern half of the study area is characterized by  
the Upper Agno River course (region 3 in Figure 1), which flows N to S, and is dammed by three cascading dams used for  
110 hydroelectric power generation: Ambuklao Dam in the North, Binga Dam in the middle, and San Roque Dam in the South. In  
the West, the study area is characterized by smooth slopes between 600 and 1500 m.a.s.l., where Baguio City and the  
Municipality of La Trinidad are located (region 1 in Figure 1). The mountainous region between Upper Agno River and the  
city and municipality in the West, in the middle of the study area, was the most affected area by Typhoon Mangkhut in 2018  
(region 2 in Figure 1). The valleys are characterized by steep slopes, with altitudes ranging from 263 to 2190 m.a.s.l. in the  
115 highest point. The municipality of Itogon is the main inhabited area in these valleys, with a population of nearly 60000  
inhabitants. Itogon is a mining town, where the extraction of gold has been one of the main economic activities since the 1990s,  
and some tailings dams can be observed in its surroundings. The bedrock of the area is mostly constituted by Cretaceous,  
Tertiary and Quaternary igneous and sedimentary rocks, part of the magmatic arc formed mainly in response to subduction  
along the Manila Trench since the early Miocene (Bellon and P. Yumul Jr., 2000). While the sedimentary bedrock consisting  
120 of limestones and clastic sedimentary rocks predominate in region 1 of the study area (Figure 1), the mountainous region in  
the centre (region 2 in Figure 1) and the eastern river plains (region 3 in Figure 1) mostly consist on diorite and diorite porphyry  
(MGB, 2006). The study area can also be described as seismically active. The whole area is covered by surficial formations  
consisting of loam and clays and undifferentiated mountain soils. Finally, the vegetative cover is mainly forest, but it also  
contains pine trees, fruit trees, shrubs and open grassland (Palangdan, 2018).

### 125 2.2 Climate

The Philippines is characterized by having several types of climate: from tropical rainforest, tropical savanna or tropical  
monsoon to humid subtropical, in higher altitudes, such as in our study area. The country is divided in 4 climatic regions, based  
on the distribution of rainfall as presented in the Modified Corona Climate Map of the Philippines (CADS/IAAS CAD and  
PAGASA/DOST, 2014). Our study area is in the Type 1 zone, characterized by having two pronounced seasons: dry from



130 November to April and wet during the rest of the year. Most rain falls between June and September. The average annual  
precipitation in our study area, during the period 1960-1990 (Hijmans et al., 2005) ranges from 3276 mm in the higher  
elevations to 1894 mm in the floodplain, with a mean value of 2766 mm. The Western and central part of the study area  
(Regions 1 and 2 in Figure 1) are characterized by having lower mean temperatures and higher amounts of rainfall. In contrast,  
135 (Table 1). The winds are controlled by two systems in the Philippines: the northeast monsoon, active from October to late  
March, and the southwest monsoon, prevalent during the months of July to September. Both monsoons bring heavy rains in  
parts of the country where the prevailing wind affects. Moreover, from the approximately 20 tropical cyclones that enter the  
Philippine area of Responsibility (PAR) every year, most of them hit northern Luzon, and seven to eight make landfall  
(Nolasco-Javier and Kumar, 2019; Yumul et al., 2011).

### 140 **2.3 Landslide activity related to previous typhoons**

Due to the frequent passage of tropical cyclones over the landslide-prone slopes of the study area, rainfall-induced landslides  
are frequent. Since 2001, at least 14 typhoons causing landslides have hit the study area, according to Nolasco-Javier and  
Kumar (2018) and Paringit et al (2020). The most devastating episodes in the last decades, before Typhoon Mangkhut, have  
been Typhoon Bilis (2006), with 53 landslides reported; Typhoon Melor and Typhoon Parma (simultaneous in 2009), with 97  
145 landslides reported and Typhoon Koppu (2015), with 80 landslides reported to the City Disaster Risk Reduction and  
Management Council (CDRRMC) of the City of Baguio.

During Multiple-Occurrence Regional Landslide Events (MORLEs), such as the ones triggered by typhoons and tropical  
storms, small or remote landslides are often unreported. Further studies from Nolasco-Javier et al (2015) and Nolasco-Javier  
150 and Kumar (2019) demonstrate that the number of landslides caused by Typhoon Parma in the area of Tublay was, by far,  
larger than the reported events. Therefore, the actual complete landslide record in the area is unknown. The rapid urbanization,  
together with the ongoing mining activity also represents a relevant factor in landslide risk in the area, though these factors are  
were not considered in this study (Mines and Geosciences Bureau, 2018).

### 155 **2.4. Typhoon Mangkhut (13-15 September 2018)**

From 13 – 15 September 2018, the study area was hit by the passage of Typhoon Mangkhut (called Typhoon Ompong in the  
Philippines; Figure 2a). The highest observed 4 day rainfall total (12 to 15 September 2018) of 794 mm in Baguio City  
PAGASA weather station was recorded due to the passage of Typhoon Mangkhut (Weather Division PAGASA, 2018). The  
estimations from the Global Precipitation Measurement mission (Huffman et al., 2019) show lower values over the larger area  
160 affected by landslides, with 360 mm of rainfall over a 44-hour period (Figure 2b). The typhoon triggered an elevated number  
of landslides in the area (Figure 1). The landslides were typically shallow translational landslides, mud and debris flows, often



with a complex behaviour: starting as a shallow landslide and becoming a flow (Varnes, 1978). However, rockslides and rockfalls were also reported. A detailed report on the landslides occurred, followed by a hazard assessment including field surveys in six barangays within critical areas, was issued by the Mines and Geosciences Bureau just after the event (Mines and Geosciences Bureau, 2018). Some of the debris flows had extraordinarily long runouts, such as the fatal landslide that killed more than 80 miners and their families in the area of Barangay Ucab, on the 15 September around 13:00 h local time, further described in the following sections of this paper.

### 3 Data and methods

#### 3.1 Compiling a landslide inventory and magnitude-frequency analysis

The first step to evaluate the preconditioning and triggering factors of the landslides triggered by Typhoon Mangkhut was the creation of a landslide inventory. We mapped landslides manually using satellite imagery by comparing pre- and post- Typhoon Mangkhut images of the study area. The sources of the satellite imagery were of diverse resolution (Table 2) and were combined with digital terrain models as well as with the use of Google Earth™ to more clearly identify the landslides. We experimented with an automatic landslide mapping tool to map landslides more efficiently, however, when comparing with visual observations, we found the success rate insufficient (Abancó et al., 2020), so the final inventory was entirely done using manual techniques.

Despite having many advantages, such as the possibility to map large and often not accessible mountain regions (Guzzetti et al., 2012), satellite mapping has some limitations, such as the availability of good images, cloud free, within a sensible time period before and after the event. In our study, high resolution images have a gap of several months (pre- and post- typhoon) (Table 2). Considering that landslides are not uncommon in the area, and that the construction and mining activities are intense, some of the landslides mapped using satellite images may not have occurred during Typhoon Mangkhut but before or after. For this reason, other imagery sources (Table 2) and Google Earth, together with the comparison with local reports reporting field surveys after the Typhoon (Mines and Geosciences Bureau, 2018) have been used to cross-check part of the inventory.

Landslides were mapped as polygons, without distinguishing source and runout areas, as it was often difficult to discriminate between slides, debris flows and earth flows as well as the transition between them. In the cases where the deposition areas were clearly differentiated from failure and runout areas, these have not been included in the polygons; however, in cases where runout was not long it was difficult to differentiate them. The dense vegetation covering a major part of the slopes was useful to identify and delineate the landslides, as they are easily visible as bare soil within a body of dense vegetation. Moreover, the Normalized Difference Vegetation Index (NDVI) proved to be useful to identify such changes.



We plotted the magnitude-frequency distribution of landslides across the study area and estimated the exponents of the tail of the resulting characteristic power law distribution using the maximum likelihood estimate procedure of Clauset et al. (2009).  
195 Finally, a more detailed analysis was done on one major landslide that occurred in the area of First gate, in Barangay Ucab (region 2 of the study area, see Figure 5), where small scale miners were staying in a Bunkhouse owned by Benguet Corporation (Palangdan, 2018). This landslide had a combined behaviour, evolving from a hillslope into a flow with a particularly long runout, that ended up in a tragedy causing the loss of life of 80 miners.

### 3.2 Analysis of landscape controls on landslides

200 In order to assess the influence of landscape characteristics on the spatial distribution of landslides, we combined the landslide inventory with topographical data and several thematic maps with terrain information using spatial analysis techniques in ArcMap 10.6.1 (ESRI, 2018). We obtained the frequency distribution for each governing factor both for the total of the study area and only for the areas affected by landslides. A 5-m resolution Digital Surface Model acquired in 2013 with IfSAR techniques (NAMRIA, 2013) provided the topographical information of the study area: elevation, slope and aspect degree.  
205 Maps on soil type (Victor A. Bato, Ozzy Boy Nicopior, 2004), land cover (NAMRIA, 2010) and bedrock geology (MGB, 2006) were used to retrieve information on further terrain factors. Bedrock geology was only available for the 63% of the study area, corresponding to the boundaries of the Baguio quadrangle geological map.

### 3.3 Analysis of rainfall and soil moisture

Rainfall data from 2018 at a resolution of 0.1 degrees (approx.. 10 km) and 30 minute time interval was acquired from the  
210 Global Precipitation Measurement (GPM IMERG) mission (Huffman et al., 2019) for the study area and its surroundings. These data are of particular interest to identify any correlation between the spatial variability of the rainfall associated with Typhoon Mangkhut and the distribution of landslides, instead of having only the point-based data from Baguio city rain gauge (Figure 2). Moreover, it enables tracking of the distribution of antecedent rainfall, and analysis of the role this played in the occurrence and distribution of landslides.

215 In order to do a more detailed analysis of the rainfall conditions that led to landsliding, the main part of the analysis was based only at one of the rainfall GPM grid points, the nearest to the fatal landslide in Barangay Ucab. The definition of the rainfall duration is a key consideration in the analysis of the rainfall thresholds for landslides, which often brings uncertainty to the analysis (Abancó et al., 2016). Frequently the information of the failure time of landslides is not exactly known, therefore the  
220 duration of the total rainfall (from the start of the rainfall until it finishes) is considered. According to the reports issued after Typhoon Mangkhut, the fatal landslide in Barangay Ucab must have taken place between 05:00 and 07:00 UTC, so in this case, the comparison between the triggering rainfall and the total rainfall was possible.



We analysed the characteristics of the triggering rainfall (Typhoon Mangkhut) as well as other high intensity rainfall events in the preceding and following months that did not trigger landslides. In order to define rainfall events, we have assumed that an event starts and ends after and before a period of 1 hour of no rain, following Abancó et al. (2016). Our selection of high intensity rainfall events was based on a criterion of 3-hour mean GPM IMERG rainfall intensity exceeding 4 mm hr<sup>-1</sup>. The selection criteria was based on the fact that only 3% of the 30 minute rainfall records from GPM IMERG exceeded the 4 mm hr<sup>-1</sup> threshold at the grid point near Barangay Ucab in 2018, therefore the 3-hour time window was considered to be a relevant filter to select high intensity rainfall events. The purpose of this analysis is to identify the characteristics of the landslide triggering rainfall by comparing it to other relevant rainfall events and to better identify the conditions that caused Typhoon Mangkhut to trigger so many landslides.

In addition to calculating antecedent rainfall in the lead up to Typhoon Mangkhut, we also analysed soil moisture data. The data are also from a satellite source, specifically from the Soil Moisture Active Passive mission (SMAP), acquired by means of a radiometer (passive) instrument and a synthetic-aperture radar (active) instrument operating with multiple polarizations in the L-band range. SMAP data have a resolution of 9 km and 3 hours. We used data between May and September 2018, from Level 4 (L4), corresponding to the surface and root zone soil moisture data (0-100 cm vertical average) in the form of volume of water/volume of terrain (Reichle et al., 2017).

## 4 Results

### 4.1 Landslide characteristics

A total of 1101 landslides were manually mapped, most of them located in the region 2 of the study area (Figure 1). The landslides in the study area have areas from 25 m<sup>2</sup> up to 120000 m<sup>2</sup>, representing a mean density of 1.9 landslides/km<sup>2</sup>, a maximum value of 4.8 landslides/km<sup>2</sup> in region 2. The fatal landslide in Barangay Ucab, is also located in region 2 and is highlighted in Figure 1. The exceedance probability distribution of the landslide areas has a characteristic roll-over and power law tail. The exponent of the power tail is 2.65, and the rollover point is located at 190 m<sup>2</sup> approximately (Figure 3).

Elevations in the study area range between 263 and 2190 m.a.s.l. (Figure 4a) and follow a distribution close to normal, with a maximum in elevations between 1101 and 1320 m.a.s.l. The landslide density is also highest within the same range, in terms of mean elevation. However, only 4 landslides occurred below 660 m.a.s.l. and only 1 over 1760 m.a.s.l. Slope gradients that favoured landslides are shifted towards higher gradients than the study area distribution, with most landslides occurring on slopes steeper than 30 degrees (Figure 4b). However, flatter areas down to 10 degrees and steeper up to 50 degrees were affected by failure of landslides too. Particularly striking is the aspect control on landsliding with a concentration of landslides on East-Southeast-South facing slopes (Figure 4e).

255



The study area is covered by mountain soils, Ambassador silt loam and Bakakeng Clay mostly. Nevertheless, landslides essentially happen in Bakakeng clay and Halsema clay loam and only to some extent in the Ambassador silt, but not in mountain soils (Figure 4c), which are mostly covered by coniferous forest and natural grasslands. Landslides mostly occurred in wooded grassland, while only a small amount take place in coniferous forests (Figure 4d). It is worth nothing that although  
260 the Halsema clay loam is scarce in the study area, the density of landslides is particularly high.

In terms bedrock geology, the area has predominantly a sedimentary sequence of basaltic and andesitic volcanic rocks (Pugo formation), followed by intrusive bodies consisting of diorites and granodiorites (Central Cordillera diorite complex) and a sequence of conglomerates, sandstone and shale (Zigzag formation). The higher density of landslides is located in the Central  
265 Cordillera Diorite Complex and the Balatoc Dacite (Figure 4f).

## 4.2 Rainfall and soil moisture conditioning and triggering of landslides

### 4.2.1 Rainfall

The GPM IMERG rainfall data measured in the study area during the passage of Typhoon Mangkhut indicates that the highest intensities, recorded at 03:30 UTC on 15 September, occurred in the eastern region of the study area (Figure 6), which also  
270 received the greatest accumulated rainfall over the course of the event (Figure 2). However, the rainfall accumulated throughout the previous two weeks (hereafter called antecedent rainfall) was higher in the central region, where most of the landslides occurred. In this central region, the antecedent rainfall was up to 245 mm (according to GPM IMERG measurements), which is still less than the rainfall accumulated during the Typhoon. The fact that the antecedent rainfall was higher in the area where most of the landslides occurred, even if the intensities were lower, suggests that the wetness of the terrain played an important  
275 role in the mechanism of failure.

A detailed analysis of rainfall and soil moisture conditions in the lead up to landslides is based on the GPM IMERG point closest to the fatal landslide at Barangay Ucab (Figure 5) for which timing is most precisely known. The Typhoon Mangkhut rainfall at this point was compared to 33 high intensity rainfall events (3-hour mean intensity above  $4 \text{ mm hr}^{-1}$ ) over the  
280 preceding and following months that did not trigger a MORLE. While Typhoon Mangkhut rainfall had a duration of 43.5 hours (34 hours until the fatal landslide in Barangay Ucab was triggered), according to the criteria of 1 hour without rainfall for the initiation and end of the event, the durations of the other high intensity rainfall events spanned from 2 to 107 hours. The rainfall that occurred during the passage of Typhoon Mangkhut was also not the highest in terms of accumulated rainfall, as the records show accumulations up to 409 mm in prior high intensity rainfall events. The comparison between the intensity-duration  
285 relationships (maximum rainfall intensity for different durations) of the high intensity rainfall events indicates that two events in 2018 had higher intensities (up to 2 hours duration and for long durations of 48 and 72 hours) than Typhoon Mangkhut (Figure 7). Both events happened earlier in the year than Typhoon Mangkhut: on 21 May and 20 July respectively.



As introduced in Section 3.3, the GPM IMERG data represents an average of the rainfall in each of the 0.1 x 0.1 degree cells, which means that even if a high peak of rainfall occurs in a cell (such as the one registered by the rain gauge at Baguio city) it is averaged above the whole area. We compared the high intensity rainfall events selected for the analysis. The results revealed that a great number of rainfall events clearly exceed global intensity-duration thresholds (Caine, 1980) and regional thresholds (Arboleda et al., 1996; Nolasco-Javier et al., 2015; Nolasco-Javier and Kumar, 2018), despite having used data from GPM IMERG, which tends to underestimate rainfall in extreme events.

#### 4.2.2 Soil moisture

The SMAP data containing information on the soil moisture on the root zone (at 0-100 cm depth) from May to September 2018 in 4 different points of the study area was analysed. As can be seen in Figure 8, soil moisture increases from May to September and the correlation with the rainfall is clear. The increments of soil moisture can be observed in two different situations: a) after a particular high intensity rainfall, such as the one occurred on 20 July (that had a higher intensity than Typhoon Mangkhut); or b) after periods of more continuous prolonged rainfall at lower intensity, for example in mid-June or early August. The increase of soil moisture with time is continuous, but especially significant from July onwards. The increase in July is especially relevant in points C and A, that were lower than B and D in May, June and early July but after this event are higher. The higher levels of soil moisture achieved in the analysed months are close to 0.455 m<sup>3</sup>/m<sup>3</sup>, which could be close to the level of full saturation limit of the soil. Typhoon Mangkhut occurred after several days of continuous rainfall, in August and early September, that kept a high continuous level of soil moisture, almost up to 0.45 m<sup>3</sup>/m<sup>3</sup>. Figure 9 shows the timeline of the rainfall and the soil moisture (in point C) during the typhoon (13 September 2018 at 21:00 UTC until 15 September 2018 15:30 UTC), with a temporal resolution of 30 minutes for the rainfall and 3 hours for the soil moisture.

## 5 Discussion

In this study, we investigate the landscape and meteorological preconditioning and triggering factors of the landslides triggered by Typhoon Mangkhut in a study area of the province of Benguet (Luzon, Philippines). The typhoon triggered an elevated number of landslides, with the highest density (4.8 landslides/km<sup>2</sup>) in the central part of the study area, around the municipality of Itogon, a region with steep slopes in the southern end of the Cordillera Central. The impact of this event was significantly high, mainly due to two main aspects: a) an elevated vulnerability of elements in the area, with an important presence of mining activity and settlements; and b) the complex behaviour of some of the landslides, with long runouts and elevated entrainment rates, which magnified their volume. We will look at landslide runout and controls on this in a separate study.

Using a landslide inventory based on a single event provides information that is strongly influenced by the event characteristics itself but may not be representative for the evaluation of the landslide hazard of the area. Systematic inventories should be



320 conducted over multiple years to provide more reliable information for the evaluation of size statistics of landslides as well as  
of the susceptibility of the landscape to landsliding (e.g.: Guzzetti et al., 2005, 2006; Del Ventisette et al., 2014). However,  
our analysis gives an indication of landslide characteristics and of the landscape controls in the region that will contribute  
towards a future landslide hazard assessment. Furthermore, it is of great importance for the understanding of the rainfall  
triggering conditions of landslides in the territory and in working towards landslide early warning in the region.

### 325 **5.1. Landslide characteristics and landscape preconditioning**

We are not aware of any magnitude-frequency distribution of landslides for the Philippines and thus we fill this gap in the  
literature here. The magnitude-frequency distribution of the areas of the landslides in the inventory shows a characteristic  
shape with rollover and power law tail, with an exponent of the power tail of 2.65 and a rollover point around 190 m<sup>2</sup>. This  
exponent is higher than two landslide distributions triggered by typhoon events in Taiwan, with exponents of 1.42-1.60 (Chien-  
330 Yuan et al., 2006), though similar to earthquake-triggered landslide inventories in China (Li et al., 2013) and Haiti (Gorum et  
al., 2013): 2.63 and 2.71 respectively (Tanyaş et al., 2019). These numbers, as 2.65 obtained in this study, suggest that the  
small landslides are more frequent than larger ones, in comparison to other studies where the exponent of the power law tail is  
lower than 2 (Bennett et al., 2012; Van Den Eeckhaut et al., 2007). Further mapping in the region and across other regions of  
the Philippines will help to refine these distributions and exponents.

335

An interesting finding of this study is the strong aspect control on landsliding in Typhoon Mangkhut. A possible explanation  
for aspect control of landslides in the literature is differences in vegetation and thus root cohesion between aspects that receive  
differing amounts of solar insolation (Rengers et al., 2016). Indeed landslides in the region occur within wooded grasslands  
and rarely in coniferous forest (Figure 4d), with higher root binding of the soils. Another possible explanation would be that  
340 these slopes have a soil type that is more prone to landslides, so the Bakakeng clay or the Halsema clay loam. This reddish-  
brown clay and the brownish clay loam are characterized by having a very slow internal drainage (low permeability) (Carating  
et al., 2014), which may explain their tendency to fail, due to an excessive pore pressure, when they are saturated. Further  
analysis on the geotechnical properties of these clayey soils should be carried out to determine what makes them more prone  
to landsliding to the other soils in the study area. For example, in high plasticity clays, their exposure to repetitive wet-dry  
345 cycles may reduce their shear strength (Khan et al., 2017); or the appearance of cracks, which may change the hydraulic  
conductivity and make them more prone to landsliding (Khan et al., 2019).

However, although landslides tended to happen in a certain land cover (wooded grasslands) and soil type (Bakakeng clay and  
Halsema clay loam), there is no evidence that this could explain the prevalent orientation of the slopes affected by landslides  
350 to the East-Southeast, as there are no distinct differences in vegetation or soil type between different aspects. Therefore, we  
suggest this trend may be better explained by the typhoon trajectory and wind directions, from East-Southeast to West-  
Northwest, with winds driving rains into windward facing slopes more intensely, whilst leeward slopes are more protected.



On one hand, in some previous studies typhoon trajectory and wind direction have not been found to play a role in typhoon triggered landslides in similar regions (e.g. Chen et al., 2019). On the other hand, other studies suggest that the wind does affect rainfall intensities on various slope aspects as the leeward sides are subjected to lower rainfall intensity than the windward sides, and therefore the occurrence of landslides can be affected by the winds (de Lima, 1990; Liu and Shih, 2013). Hence, the topic deserves further research.

Although in this study we have not considered anthropogenic factors, local reports (Mines and Geosciences Bureau, 2018) and studies (Nolasco-Javier and Kumar, 2018) have pointed out that rapid urbanization and mining activities can severely impact the susceptibility of the slopes to landsliding. The presence of underground mines in the region, summed to the existence of faults and fractures in the bedrock, generates a labyrinth of underground excavations that may clearly affect the slope stability and could be looked at in further research.

## 5.2. Rainfall and soil moisture conditions leading to landsliding

The analysis of 2018 rainfall in the study region shows that more rainfall intensity does not mean more landslides, in contrast to some other studies (Chen et al., 2013; Lin and Chen, 2012). In fact, the results of this study do not support the model proposed by Crozier (2017), that suggests a higher density of landslides at the core of the rainfall intensity cell, decreasing as the rainfall intensity does. Instead, the density of landslides was higher in areas of greater antecedent rainfall, supporting the findings of Nolasco-Javier and Kumar (2018) in the same region. However, whilst Nolasco-Javier and Kumar (2018) suggested a threshold of 500 mm of rainfall accumulated over the rainy season is needed for landsliding, we suggest that the threshold is far higher. The 500 mm threshold was already reached in our study area on the 14 June 2018, yet a very intense event in July and some other intense rainfalls failed to trigger landslides according to the records and the satellite imagery available. Our study suggests a threshold of 2600 mm of rainfall accumulated over the rainy season for landsliding to occur. This demonstrates the difficulty of defining thresholds based on rainfall for a given area and the need for multiple events to refine thresholds. Furthermore, multiple rainfall events exceeded the global threshold Caine (1980). This is probably because such thresholds are obtained using a high diversity of meteorological patterns, therefore may be too low for extreme climates such as tropical in the Philippines.

Soil moisture data provides an even more accurate picture of the soil conditions at the time of landsliding than antecedent rainfall data. There are several studies that have started to combine soil moisture with rainfall data to define landslide thresholds (Hürlimann et al., 2019; Mirus et al., 2018) and for landslide early warning (e.g.: Kirschbaum and Stanley, 2018; Krogli et al., 2018). The analysis of soil moisture in our study area in the lead up to Typhoon Mangkhut shows that the volumetric water content of the soil increased over the rainy season, reaching a maximum of  $0.455 \text{ m}^3/\text{m}^3$ , when the typhoon happened in September 2018. This value is actually a reasonable value for the porosity of clays, which would suggest that it may correspond



to the saturation point of Bakakeng clay. Therefore, any rainfall occurring in these saturated conditions would create an increase of soil pore-water pressure, which would result in a decrease of effective stress and therefore a tendency to fail.

### 5.3. Potential of satellite-based rainfall and soil moisture data for landslide early warning

390 In order to explore the potential of satellite-based rainfall and soil moisture data for landslide early warning, we conducted a further analysis of rainfall and soil moisture conditions for the 34 high intensity rainfalls (including Typhoon Mangkhut) (Figure 10). Although Typhoon Mangkhut rainfall shows one of the highest values of volumetric water content in the soil and also has high values for all four rainfall parameters analysed (mean rainfall, peak rainfall intensity, rainfall duration and total rainfall of the event), it does not clearly stand out from other rainfalls. This may be because there are other factors involved in  
395 landsliding that we have not considered here, such as the atmospheric pressure (Pelascini et al., 2020) or the wind directions, linked to the Typhoon trajectory. Alternatively, it may be that satellite-based rainfall and soil moisture data do not adequately capture the conditions on the ground. Hence, satellite-based data should be used with caution in landslide early warning systems (Hidayat et al., 2019; Kirschbaum and Stanley, 2018), ensuring that threshold curves are derived using the same source of data (Brunetti et al., 2018).

400

Further work should be carried out in the region in order to establish a reliable threshold to identify and provide reliable early warning of landslide-triggering rainfalls, using either rain gauges or satellite rainfall products or a combination. The high temporal resolution of satellite data allows more detailed thresholds, which would be more useful to be applied in early warning systems, than daily values, such as the ones suggested by Nolasco-Javier and Kumar (2018) and Nolasco-Javier et al. (2015).  
405 However, it is also important to consider the uncertainty that the satellite data brings compared to in-situ measurements. Hence, we are working on the installation of in-situ sensors to verify satellite data. A combination of satellite rainfall and soil moisture data (in real time or forecasted) with rain gauges and soil-moisture sensors could potentially be combined in a future landslide early warning system.

## 6 Conclusions

410 We used satellite imagery to produce a complete inventory of landslides triggered by Typhoon Mangkhut (2018), which contains 1101 landslides. The magnitude-frequency distribution of the landslide areas, the first we are aware of for the Philippines, has a characteristic rollover effect, with a power law tail, with an exponent of 2.65. The exponent is higher than in other typhoon-triggered landslide inventories, which suggests that bigger landslides are rarer in the study area.

415 The geomorphological analysis of the inventory shows that most of the landslides happen face East-South East. After discarding land cover or soil type related explanations, we suggest this is somehow controlled by the trajectory of the typhoon and wind directions, from East-Southeast to West-Northwest. Landslides occurred predominantly in Bakakeng clay and



420 Halsema clay loam, two clayey soils that cover some slopes in the study area, which have a low permeability. Another factor  
that may have played a role in the distribution of landslides but was not considered in this research is extensive mining activities  
in the region, associated to the excavation of many interconnected underground mines over the study area, and the increasing  
infrastructure, which generates overloads in the slopes.

425 We used GPM IMERG rainfall data to analyse the spatial distribution of the rainfall associated to Typhoon Mangkhut.  
Antecedent rainfall in the two weeks leading up to the typhoon better explains the spatial landslide pattern than rainfall  
intensity. This result suggests, as pointed out by other studies, that the soil moisture may play a very important role in the  
trigger of landslides in the area. We used SMAP-L4 soil moisture data to analyse the soil moisture evolution along the rainy  
season of 2018. The results show that soil moisture increased along the season, achieving highest values (probably at the  
saturation point) when Typhoon Mangkhut hit the area. However, in previous months, other intense rainfalls happened, also  
with high volumetric water content, that did not trigger landslides.

430 The Typhoon Mangkhut rainfall was compared to 33 other high intensity rainfalls occurred in 2018 and to some published  
global and regional rainfall thresholds. Firstly, of this analysis was that, although satellite-based rainfall products tend to  
underestimate rainfall measurements, a great number of rainfall events (that did not trigger landslides) were above global and  
regional rainfall thresholds used for comparison. The need of further analysis of landslide triggering rainfall in the area is  
435 highlighted, preferably including a comparison with ground-based measurements.

440 Finally, we did a preliminary analysis to foresee the potential of combining triggering rainfall and the soil moisture data to be  
used in a potential early warning system. We find that it is difficult to isolate Typhoon Mangkut from other rainfall events that  
happened in the lead up to the typhoon with higher intensities and under equally saturated soil conditions, yet did not trigger  
landslides. The results show that it is not possible to draw a threshold only using one single landslide triggering event and  
point out that the exclusive use of satellite data may induce some uncertainties due to the area-averaged measurements, which  
need to be analysed in future studies.

### Code/Data availability

445 The landslide inventory will be available at the end of the SCaRP project (currently January 2022), and will be accessible at  
NERC Environmental Information Data Centre EIDC <https://eidc.ac.uk/deposit>. In the meantime, anyone interested in a  
collaboration using the data may contact the corresponding author.



### Author contribution

450 GB and CA designed the study. CA mapped the landslides, analysed the data (geomorphological, rainfall and soil moisture) and led the writing of the article with contributions from GB. AM provided GPM IMERG rainfall data and contributed in the analysis of this. MM and FT provided information on the Mangkhut event and contributed in the collection of geomorphological data. All authors contributed in the writing and gave final approval of this manuscript.

### Competing interests

The authors declare that no competing interests are present.

### 455 Acknowledgments

We are thankful to Goddard Space Flight Center, Precipitation Measurement Missions at the National Aeronautics and Space Administration (NASA) and the National Snow and Ice Data Centre respectively for making GPM IMERG and SMAP datasets freely available. David Hein-Griggs is thanked for his support in the extraction and processing of SMAP-L4 data.

460 We are also grateful to the Mines and Geosciences Bureau (MGB) for providing the Geological Map from Baguio region, the Philippine Atmospheric, Geophysical and Astronomical Services Administration (PAGASA) for providing the rainfall data of the Baguio rain gauge and to Xavier Fuentes for making the soil and land cover data available through PhilGIS.org. The researchers based in the UK (C. Abancó, G. Bennett and A.J. Matthews) are funded by NERC Newton Agham fund (contract NE/S003371/1 Project SCaRP) and the researchers based in the Philippines (M. Matera and F. Tan) are funded by the Department of Science and Technology – Philippine Council for Industry, Energy, and Emerging Technology Research and  
465 Development (DOST-PCIEERD, Project No. 07166).



## References

- Abancó, C., Hürlimann, M., Moya, J. and Berenguer, M.: Critical rainfall conditions for the initiation of torrential flows. Results from the Rebaixader catchment (Central Pyrenees), *J. Hydrol.*, 541, 218–229, doi:10.1016/j.jhydrol.2016.01.019, 2016.
- 470 Abancó, C., Bennett, G., Briant, J. and Battiston, S.: Towards an automatic landslide mapping tool based on satellite imagery and geomorphological parameters . A study of the Itogon area ( Philippines ) after Typhoon Mangkhut, , 0–1, 2020.
- Alvioli, M., Mondini, A. C., Fiorucci, F., Marchesini, I. and Alvioli, M.: Automatic landslide mapping from satellite imagery with a topography-driven thresholding algorithm, , (MI), 1–7, doi:10.7287/peerj.preprints.27067v2, 2018.
- Arboleda, R., Martinez, M., Newhall, C. and Punongbayan, R.: 1992 lahars in the Pasig-Potrero river system, in *Fire and mud: eruptions and lahars of Mount Pinatubo*, edited by P. R. Newhall CG, pp. 85–102, Philippine Institute of Volcanology and Seismology and University of Washington Press, Philippines,., 1996.
- 475 Bellon, H. and P. Yumul Jr., G.: Mio-Pliocene magmatism in the Baguio mining district (Luzon, Philippines): Age clues to its geodynamic setting, *Comptes Rendus l'Academie Sci. - Ser. Ila Sci. la Terre des Planetes*, 331(4), 295–302, doi:10.1016/S1251-8050(00)01415-4, 2000.
- 480 Bennett, G. L., Molnar, P., Eisenbeiss, H. and McArdell, B. W.: Erosional power in the Swiss Alps: characterization of slope failure in the Illgraben, *Earth Surf. Process. Landforms*, 37(15), 1627–1640, doi:10.1002/esp.3263, 2012.
- Bogaard, T. A. and van Asch, T. W. J.: The role of the soil moisture balance in the unsaturated zone on movement and stability of the Beline landslide, France, *Earth Surf. Process. Landforms*, 27(11), 1177–1188, doi:10.1002/esp.419, 2002.
- Borghuis, A. M., Chang, K. and Lee, H. Y.: Comparison between automated and manual mapping of typhoon-triggered landslides from SPOT-5 imagery, *Int. J. Remote Sens.*, 28(8), 1843–1856, doi:10.1080/01431160600935638, 2007.
- 485 Brunetti, M. T., Peruccacci, S., Rossi, M., Luciani, S., Valigi, D. and Guzzetti, F.: Rainfall thresholds for the possible occurrence of landslides in Italy, *Nat. Hazards Earth Syst. Sci.*, 10(3), 447–458, doi:10.5194/nhess-10-447-2010, 2010.
- Brunetti, M. T., Melillo, M., Peruccacci, S., Ciabatta, L. and Brocca, L.: How far are we from the use of satellite rainfall products in landslide forecasting?, *Remote Sens. Environ.*, 210(June 2017), 65–75, doi:10.1016/j.rse.2018.03.016, 2018.
- 490 CADS/IAAS CAD and PAGASA/DOST: Climate Map of the Philippines (1951-2010), 2014.
- Caine, N.: The rainfall intensity-duration control of shallow landslides and debris flows, *Geogr. Ann.*, 62A, 23–27 [online] Available from: [http://links.jstor.org/sici?sici=0435-3676\(1980\)62:1/2%3C23:TRIDCO%3E2.0.CO;2-H](http://links.jstor.org/sici?sici=0435-3676(1980)62:1/2%3C23:TRIDCO%3E2.0.CO;2-H), 1980.
- Carating, R. B., Galanta, R. G. and Bacatio, C. D.: *The Soils of the Philippines*, Dordrecht., 2014.
- Cawis, R. M. M.: Itogon to commemorate “Ompong” tragedy anniversary with rituals, [online] Available from: <https://pia.gov.ph/news/articles/1027251> (Accessed 24 June 2020), 2019.
- 495 Chen, Y. C., Chang, K. T., Chiu, Y. J., Lau, S. M. and Lee, H. Y.: Quantifying rainfall controls on catchment-scale landslide erosion in Taiwan, *Earth Surf. Process. Landforms*, 38(4), 372–382, doi:10.1002/esp.3284, 2013.
- Chen, Y. C., Chang, K. T., Wang, S. F., Huang, J. C., Yu, C. K., Tu, J. Y., Chu, H. J. and Liu, C. C.: Controls of preferential



- orientation of earthquake- and rainfall-triggered landslides in Taiwan's orogenic mountain belt, *Earth Surf. Process. Landforms*, 44(9), 1661–1674, doi:10.1002/esp.4601, 2019.
- 500 Chien-Yuan, C., Fan-Chieh, Y., Sheng-Chi, L. and Kei-Wai, C.: Discussion of landslide self-organized criticality and the initiation of debris flow, *Earth Surf. Process. Landforms*, 32(July), 197–209, doi:10.1002/esp, 2006.
- Clauset, A., Shalizi, C. R. and Newman, M. E. J.: Power-law distributions in empirical data, *SIAM Rev.*, 51(4), 661–703, doi:10.1137/070710111, 2009.
- 505 Crosta, G. B. and Dal Negro, P.: Observations and modelling of soil slip-debris flow initiation processes in pyroclastic deposits: the Sarno 1998 event, *Nat. Hazards Earth Syst. Sci.*, 3, 53–69, doi:10.5194/nhess-3-53-2003, 2003.
- Crozier, M. J.: Multiple-occurrence regional landslide events in New Zealand: hazard management issues, *Landslides*, 2, 247–256 [online] Available from: <http://link.springer.com/article/10.1007/s10346-005-0019-7>, 2005.
- Crozier, M. J.: A proposed cell model for multiple-occurrence regional landslide events: Implications for landslide susceptibility mapping, *Geomorphology*, 295(July), 480–488, doi:10.1016/j.geomorph.2017.07.032, 2017.
- 510 Van Den Eeckhaut, M., Poesen, J., Govers, G., Verstraeten, G. and Demoulin, A.: Characteristics of the size distribution of recent and historical landslides in a populated hilly region, *Earth Planet. Sci. Lett.*, 256(3–4), 588–603, doi:10.1016/j.epsl.2007.01.040, 2007.
- ESRI: ArcGIS Desktop version 10.6.1 user guide, 2018.
- 515 Fell, R., Corominas, J., Bonnard, C., Cascini, L., Leroi, E., Savage, W. Z. and on behalf of the JTC-1 Joint Technical Committee on Landslides: Guidelines for landslide susceptibility, hazard and risk zoning for land use planning, *Eng. Geol.*, 102, 99–111, 2008.
- Godt, J. W., Baum, R. L., Savage, W. Z., Salciarini, D., Schulz, W. H. and Harp, E. L.: Transient deterministic shallow landslide modeling: Requirements for susceptibility and hazard assessments in a GIS framework, *Eng. Geol.*, 102(3–4), 214–226 [online] Available from: <http://www.sciencedirect.com/science/article/B6V63-4T3VR9T-1/2/11ef20cb191eb274131c7008a5f06214>, 2008.
- 520 Gorum, T., van Westen, C. J., Korup, O., van der Meijde, M., Fan, X. and van der Meer, F. D.: Complex rupture mechanism and topography control symmetry of mass-wasting pattern, 2010 Haiti earthquake, *Geomorphology*, 184, 127–138, doi:10.1016/j.geomorph.2012.11.027, 2013.
- 525 Guzzetti, F., Reichenbach, P., Cardinali, M., Galli, M. and Ardizzone, F.: Probabilistic landslide hazard assessment at the basin scale, *Geomorphology*, 72(1–4), 272–299 [online] Available from: <http://www.sciencedirect.com/science/article/B6V93-4GWBDMD-1/2/28844fe2310ad51e6776d0582f37be14>, 2005.
- Guzzetti, F., Galli, M., Reichenbach, P., Ardizzone, F. and Cardinali, M.: Landslide hazard assessment in the Collazzone area, Umbria, central Italy, *Nat. Hazards Earth Syst. Sci.*, 6(1), 115–131, doi:10.5194/nhess-6-115-2006, 2006.
- 530 Guzzetti, F., Peruccacci, S., Rossi, M. and Stark, C. P.: Rainfall thresholds for the initiation of landslides in central and southern Europe, *Meteorol. Atmos. Phys.*, 98(3–4), 239–267, doi:10.1007/s00703-007-0262-7, 2007.
- Guzzetti, F., Mondini, A. C., Cardinali, M., Fiorucci, F., Santangelo, M. and Chang, K. T.: Landslide inventory maps: New



- tools for an old problem, *Earth-Science Rev.*, 112(1–2), 42–66, doi:10.1016/j.earscirev.2012.02.001, 2012.
- 535 Guzzetti, F., Gariano, S. L., Peruccacci, S., Brunetti, M. T., Marchesini, I., Rossi, M. and Melillo, M.: Geographical landslide early warning systems, *Earth-Science Rev.*, 200(October 2019), 102973, doi:10.1016/j.earscirev.2019.102973, 2020.
- Hidayat, R., Sutanto, S. J., Hidayah, A., Ridwan, B. and Mulyana, A.: Development of a landslide early warning system in Indonesia, *Geosci.*, 9(10), 1–17, doi:10.3390/geosciences9100451, 2019.
- Hijmans, R. J., Cameron, S. E., Parra, J. L., Jones, P. G. and Jarvis, A.: Very high resolution interpolated climate surfaces for global land areas, *Int. J. Climatol.*, 25(15), 1965–1978, doi:10.1002/joc.1276, 2005.
- 540 Huffman, G. J., Bolvin, D. T., Nelkin, E. J. and Tan, J.: Integrated Multi-satellite Retrievals for GPM (IMERG), version 06 NASA’s Precipitation Processing Center., *J. ISMAC*, 01(02), doi:10.36548/jismac.2019.2, 2019.
- Hürlimann, M., Oorthuis, R., Abancó, C., Carleo, L. and Moya, J.: Monitoring of rainfall and infiltration at the Rebaixader catchment (Central Pyrenees), in *7th International Conference on Debris-Flow Hazards Mitigation*, p. in press, Boulder, CO., 2019.
- 545 Khan, M. A., Hossain, M. S., Khan, M. S., Samir, S. and Aramoon, A.: Impact of wet-dry cycles on the shear strength of high plastic clay based on direct shear testing, *Geotech. Spec. Publ.*, (GSP 280), 615–622, doi:10.1061/9780784480472.065, 2017.
- Khan, S., Ivoke, J. and Nobahar, M.: Coupled effect of wet-dry cycles and rainfall on highway slope made of yazoo clay, *Geosci.*, 9(8), doi:10.3390/geosciences9080341, 2019.
- Kirschbaum, D. and Stanley, T.: Satellite-Based Assessment of Rainfall-Triggered Landslide Hazard for Situational  
550 Awareness, *Earth’s Futur.*, 6(3), 505–523, doi:10.1002/2017EF000715, 2018.
- Kirschbaum, D., Stanley, T. and Zhou, Y.: Spatial and temporal analysis of a global landslide catalog, *Geomorphology*, 249, 4–15, doi:10.1016/j.geomorph.2015.03.016, 2015.
- Krogli, I. K., Devoli, G., Colleuille, H., Boje, S., Sund, M. and Engen, I. K.: The Norwegian forecasting and warning service for rainfall- and snowmelt-induced landslides, *Nat. Hazards Earth Syst. Sci.*, 18(5), 1427–1450, doi:10.5194/nhess-18-1427-  
555 2018, 2018.
- Lagmay, A. M. F., Racoma, B. A., Aracan, K. A., Alconis-Ayco, J. and Saddi, I. L.: Disseminating near-real-time hazards information and flood maps in the Philippines through Web-GIS, *J. Environ. Sci.*, 59, 13–23, doi:10.1016/j.jes.2017.03.014, 2017.
- Leonarduzzi, E. and Molnar, P.: Data limitations and potential of hourly and daily rainfall thresholds for shallow landslides,  
560 *Nat. Hazards Earth Syst. Sci. Discuss.*, (April), 1–25, doi:10.5194/nhess-2020-125, 2020.
- Li, W. le, Huang, R. qiu, Xu, Q. and Tang, C.: Rapid susceptibility mapping of co-seismic landslides triggered by the 2013 Lushan Earthquake using the regression model developed for the 2008 Wenchuan Earthquake, *J. Mt. Sci.*, 10(5), 699–715, doi:10.1007/s11629-013-2786-2, 2013.
- Liao, Z., Hong, Y., Wang, J., Fukuoka, H., Sassa, K., Karnawati, D. and Fathani, F.: Prototyping an experimental early warning  
565 system for rainfall-induced landslides in Indonesia using satellite remote sensing and geospatial datasets, *Landslides*, 7(3), 317–324, doi:10.1007/s10346-010-0219-7, 2010.



- de Lima, J. L. M. P.: The effect of oblique rain on inclined surfaces: A nomograph for the rain-gauge correction factor, *J. Hydrol.*, 115(1–4), 407–412, doi:10.1016/0022-1694(90)90218-M, 1990.
- Lin, G. W. and Chen, H.: The relationship of rainfall energy with landslides and sediment delivery, *Eng. Geol.*, 125, 108–118, doi:10.1016/j.enggeo.2011.11.010, 2012.
- Liu, J. K. and Shih, P. T. Y.: Topographic correction of Wind-Driven rainfall for landslide analysis in central Taiwan with validation from Aerial and satellite optical images, *Remote Sens.*, 5(6), 2571–2589, doi:10.3390/rs5062571, 2013.
- Malamud, B. D., Turcotte, D. L., Guzzetti, F. and Reichenbach, P.: Landslide inventories and their statistical properties, *Earth Surf. Process. Landforms*, 29(6), 687–711, doi:10.1002/esp.1064, 2004.
- 575 Marino, P., Peres, D. J., Cancelliere, A., Greco, R. and Bogaard, T. A.: Soil moisture information can improve shallow landslide forecasting using the hydrometeorological threshold approach, *Landslides*, (December 2019), doi:10.1007/s10346-020-01420-8, 2020.
- Martino, S., Antonielli, B., Bozzano, F., Caprari, P., Discenza, M. E., Esposito, C., Fiorucci, M., Iannucci, R., Marmoni, G. M. and Schilirò, L.: Landslides triggered after the 16 August 2018 Mw 5.1 Molise earthquake (Italy) by a combination of  
580 intense rainfalls and seismic shaking, *Landslides*, 17(5), 1177–1190, doi:10.1007/s10346-020-01359-w, 2020.
- Mazzoglio, P., Laio, F., Balbo, S., Boccardo, P. and Disabato, F.: Improving an Extreme Rainfall Detection System with GPM IMERG data, *Remote Sens.*, 11(6), 677, doi:10.3390/rs11060677, 2019.
- MGB: Geological Map of Baguio City Quadrangle (1:50000), 2006.
- Mines and Geosciences Bureau: Report on the Result of the Geohazard Assessments in the Small Scale Mining Areas in the  
585 Municipality of Itogon, Benguet Province Re: Rain-Induced Landslide Incidents due to Typhoon Ompong., 2018.
- Mirus, B. B., Becker, R. E., Baum, R. L. and Smith, J. B.: Integrating real-time subsurface hydrologic monitoring with empirical rainfall thresholds to improve landslide early warning, *Landslides*, 15(10), 1909–1919, doi:10.1007/s10346-018-0995-z, 2018.
- NAMRIA: Land Cover Map, 2010.
- 590 NAMRIA: The Philippine IfSAR Project, 2013.
- Nikolopoulos, E., Borga, M., Creutin, J. and Marra, F.: Estimation of debris flow triggering rainfall: Influence of rain gauge density and interpolation methods, *Geomorphology* [online] Available from: <http://www.sciencedirect.com/science/article/pii/S0169555X15002482> (Accessed 25 August 2015), 2015.
- Nolasco-Javier, D. and Kumar, L.: Deriving the rainfall threshold for shallow landslide early warning during tropical cyclones: a case study in northern Philippines, *Nat. Hazards*, 90(2), 921–941, doi:10.1007/s11069-017-3081-2, 2018.
- 595 Nolasco-Javier, D. and Kumar, L.: Frequency ratio landslide susceptibility estimation in a tropical mountain region, *Int. Arch. Photogramm. Remote Sens. Spat. Inf. Sci. - ISPRS Arch.*, 42(3/W8), 173–179, doi:10.5194/isprs-archives-XLII-3-W8-173-2019, 2019.
- Nolasco-Javier, D., Kumar, L. and Tengenociang, A. M. P.: Rapid appraisal of rainfall threshold and selected landslides in  
600 Baguio, Philippines, *Nat. Hazards*, 78(3), 1587–1607, doi:10.1007/s11069-015-1790-y, 2015.



- Palangdan, V. T.: Save, recovery and development of Itogon. A Rehabilitation and recovery plan of the municipality of Itogon, Benguet (2019-2028), 2018.
- Papa, M. N., Medina, V., Ciervo, F. and Bateman, A.: Derivation of critical rainfall thresholds for shallow landslides as a tool for debris flow early warning systems, *Hydrol. Earth Syst. Sci.*, 17(10), 4095–4107, doi:10.5194/hess-17-4095-2013, 2013.
- 605 Paringit, M. C. R., Cutora, M. D. L., Santiago, E. H. and Adajar, M. A. Q.: Assessment of Landslide Susceptibility: a Case Study of Carabao Mountain in Baguio City, *Int. J. GEOMATE*, 19(71), doi:10.21660/2020.71.9261, 2020.
- Parker, R. N., Densmore, A. L., Rosser, N. J., De Michele, M., Li, Y., Huang, R., Whadcoat, S. and Petley, D. N.: Mass wasting triggered by the 2008 Wenchuan earthquake is greater than orogenic growth, *Nat. Geosci.*, 4(7), 449–452, doi:10.1038/ngeo1154, 2011.
- 610 Pelascini, L., Steer, P., Longuevergne, L. and Lague, D.: The impact of atmospheric pressure change and rainfall for triggering landslides during weather events, in *EGU General Assembly 2020*, pp. 0–1, On-line. [online] Available from: <https://doi.org/10.5194/egusphere-egu2020-5423>, 2020, 2020.
- Petley, D.: Global patterns of loss of life from landslides, *Geology*, 40(10), 927–930, 2012.
- Petley, D.: Drone images of the Barangay Ucab landslide, *Landslide Blog* [online] Available from: <https://blogs.agu.org/landslideblog/2018/09/18/barangay-ucab-landslide/> (Accessed 29 May 2020), 2018.
- 615 Reichle, R., G. De Lannoy, R., Koster, D., Crow, W. T. and Kimball, J. S.: SMAP L4 9 km EASE-Grid Surface and Root Zone Soil Moisture Geophysical Data, Version 3, 2017.
- Rengers, F. K., McGuire, L. A., Coe, J. A., Kean, J. W., Baum, R. L., Staley, D. M. and Godt, J. W.: The influence of vegetation on debris-flow initiation during extreme rainfall in the northern Colorado Front Range, *Geology*, 44(10), 823–826, doi:10.1130/G38096.1, 2016.
- 620 Scheip, C. M. and Wegmann, K. W.: HazMapper : A global open-source natural hazard mapping application in Google Earth Engine, , (April), 1–25, 2020.
- Segoni, S., Piciullo, L. and Gariano, S. L.: A review of the recent literature on rainfall thresholds for landslide occurrence, *Landslides*, 15(8), 1483–1501, doi:10.1007/s10346-018-0966-4, 2018.
- 625 Shu, H., Hürlimann, M., Molowny-Horas, R., González, M., Pinyol, J., Abancó, C. and Ma, J.: Relation between land cover and landslide susceptibility in Val d’Aran, Pyrenees (Spain): Historical aspects, present situation and forward prediction, *Sci. Total Environ.*, 693, 133557, doi:https://doi.org/10.1016/j.scitotenv.2019.07.363, 2019.
- Tanyaş, H., van Westen, C. J., Allstadt, K. E. and Jibson, R. W.: Factors controlling landslide frequency–area distributions, *Earth Surf. Process. Landforms*, 44(4), 900–917, doi:10.1002/esp.4543, 2019.
- 630 Tseng, C. M., Lin, C. W., Dalla Fontana, G. and Tarolli, P.: The topographic signature of a major typhoon, *Earth Surf. Process. Landforms*, 40(8), 1129–1136, doi:10.1002/esp.3708, 2015.
- Varnes, D. J.: Slope movements types and processes. Landslides analysis and control transportation research board, *Natl. Acad. Sci. Spec. Rep.*, 176(Chapter 2), 11–33, 1978.
- Del Ventisette, C., Righini, G., Moretti, S. and Casagli, N.: Multitemporal landslides inventory map updating using spaceborne



- 635 SAR analysis, *Int. J. Appl. Earth Obs. Geoinf.*, 30(1), 238–246, doi:10.1016/j.jag.2014.02.008, 2014.  
Victor A. Bato, Ozzy Boy Nicopior, B.: PhilSoil Project, 2004.  
De Vita, P., Reichenbach, P., Bathurst, J. C., Borga, M., Crosta, G., Crozier, M. J., Glade, T., Guzzetti, F., Hansen, A. and Wasowski, J.: Rainfall-triggered landslides: a reference list, *Environ. Geol.*, 35(2–3), 219–233, 1998.  
Weather Division PAGASA: Typhoon Ompong (Mangkut / 1822), 2018.
- 640 Yumul, G. P., Cruz, N. A., Servando, N. T. and Dimalanta, C. B.: Extreme weather events and related disasters in the Philippines, 2004-08: A sign of what climate change will mean?, *Disasters*, 35(2), 362–382, doi:10.1111/j.1467-7717.2010.01216.x, 2011.



645 **Tables**

**Table 1: Average maximum and minimum monthly precipitation (from 1960 to 1990) in the different regions of the study area (see Fig.1). Source: <https://www.worldclim.org/>, version 1.4, release 3.**

Month	Region 1		Region 2		Region 3	
	Average max precipitation (mm)	Average min precipitation (mm)	Average max precipitation (mm)	Average min precipitation (mm)	Average max precipitation (mm)	Average min precipitation (mm)
January	22	3	<b>30</b>	3	18	3
February	19	2	<b>22</b>	2	17	2
March	<b>50</b>	30	46	23	45	29
April	<b>115</b>	68	101	63	109	69
May	247	190	<b>265</b>	219	256	203
June	385	249	<b>432</b>	337	417	310
July	610	346	617	331	<b>635</b>	379
August	685	415	<b>783</b>	546	739	506
September	487	307	<b>586</b>	388	556	351
October	316	165	<b>335</b>	197	329	217
November	174	65	<b>192</b>	55	170	65
December	58	20	<b>78</b>	13	55	20

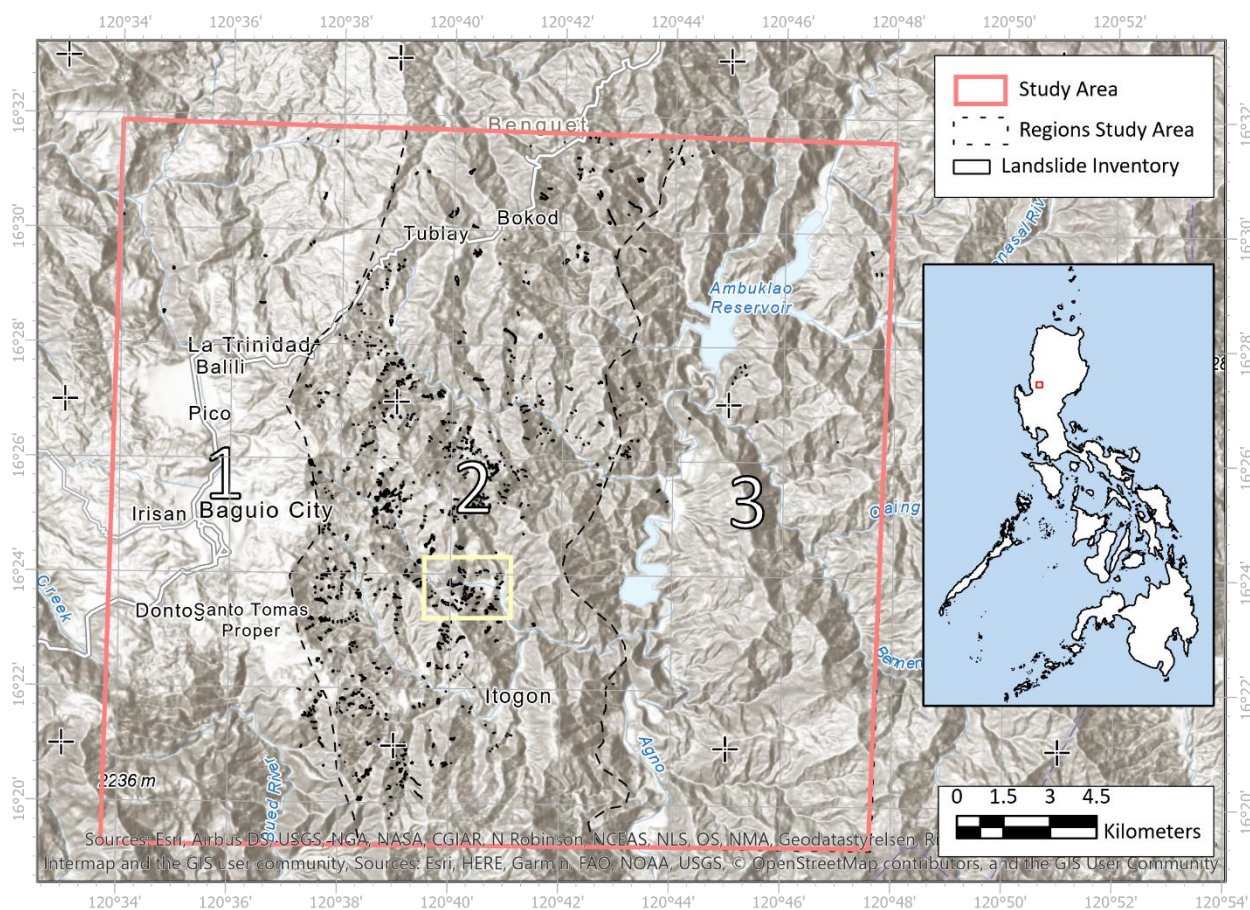
**Table 2: Details of the satellite imagery sources used in this study.**

Imagery source	Spatial resolution (m)	Data image pre-typhoon	Date image post-typhoon
WorldView2	0.5	18/02/2018	02/03/2019
Sentinel 2	10	28/04/2018	09/11/2018
Planet Labs	3	01/08/2018	21/09/2018

650



## Figures



655 **Figure 1: Landslide inventory.** Area affected by 1096 landslides triggered by Typhoon Mangkhut was mapped using polygons. Three regions of the study area are distinguished (see text). The yellow area is referred in Figure 5. Inset, location of the study area within the Philippines, in the province of Benguet (Luzon).



660

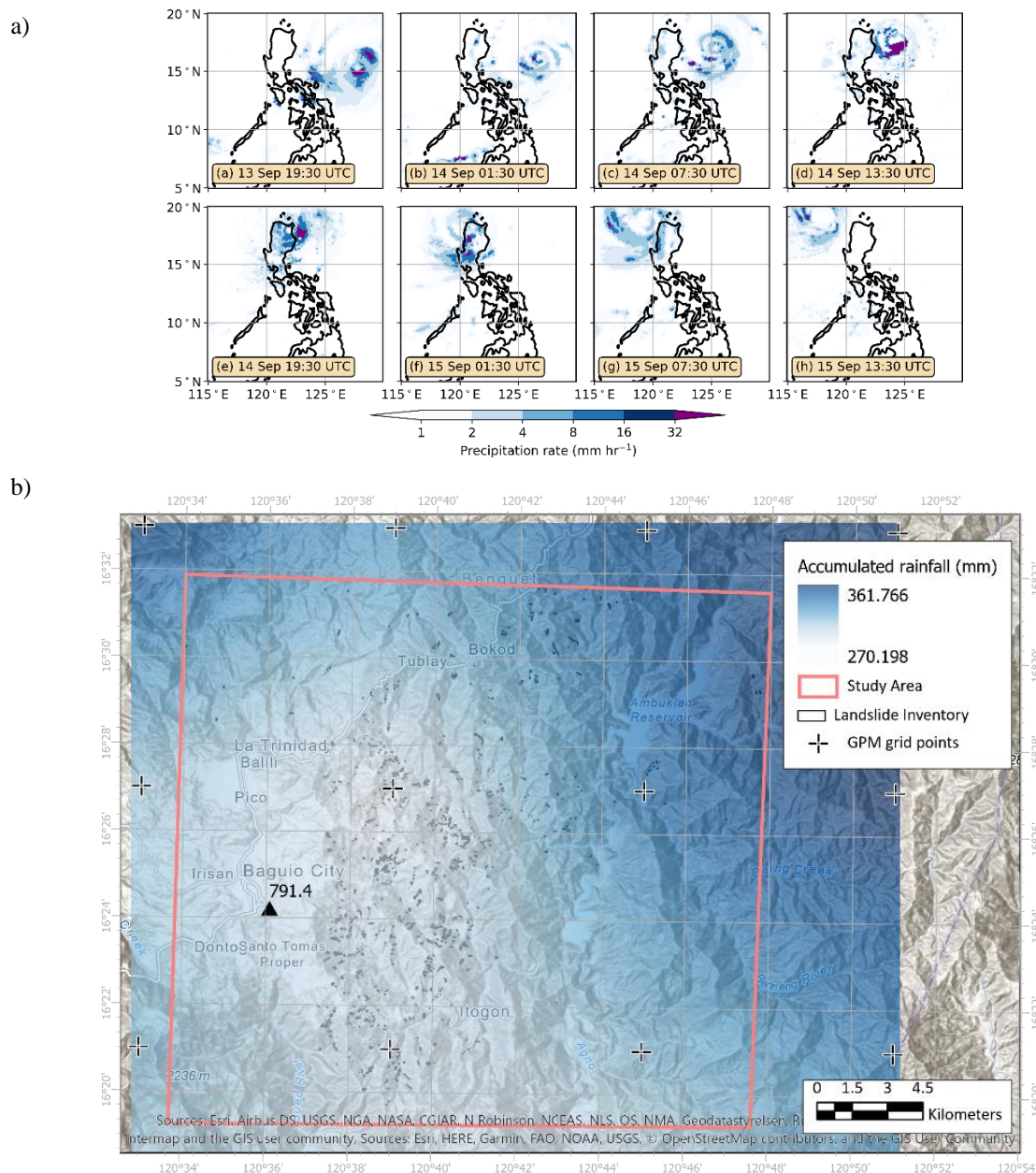
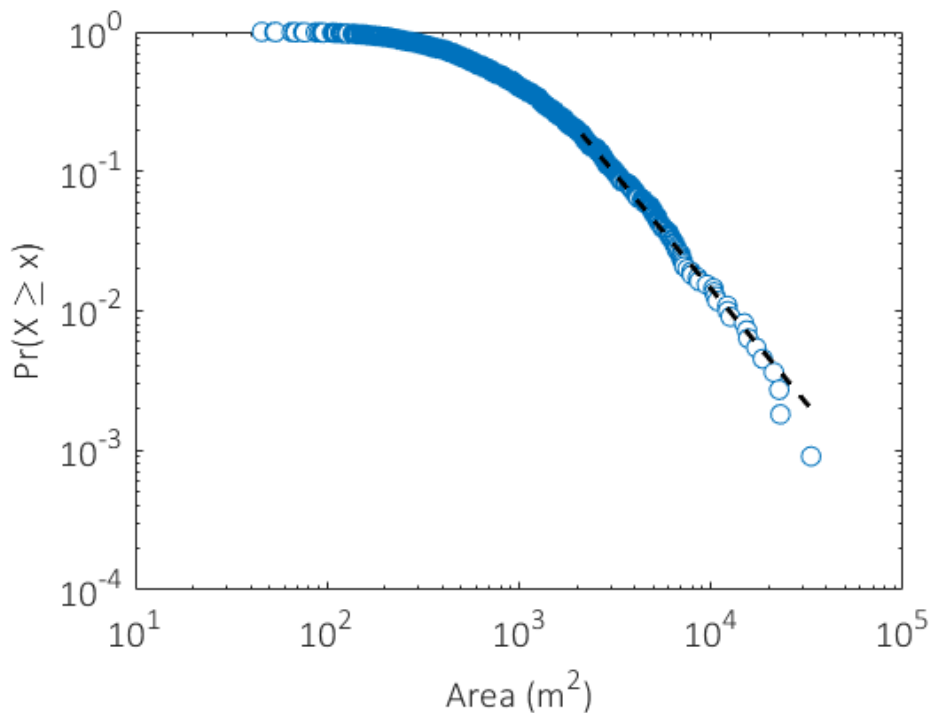
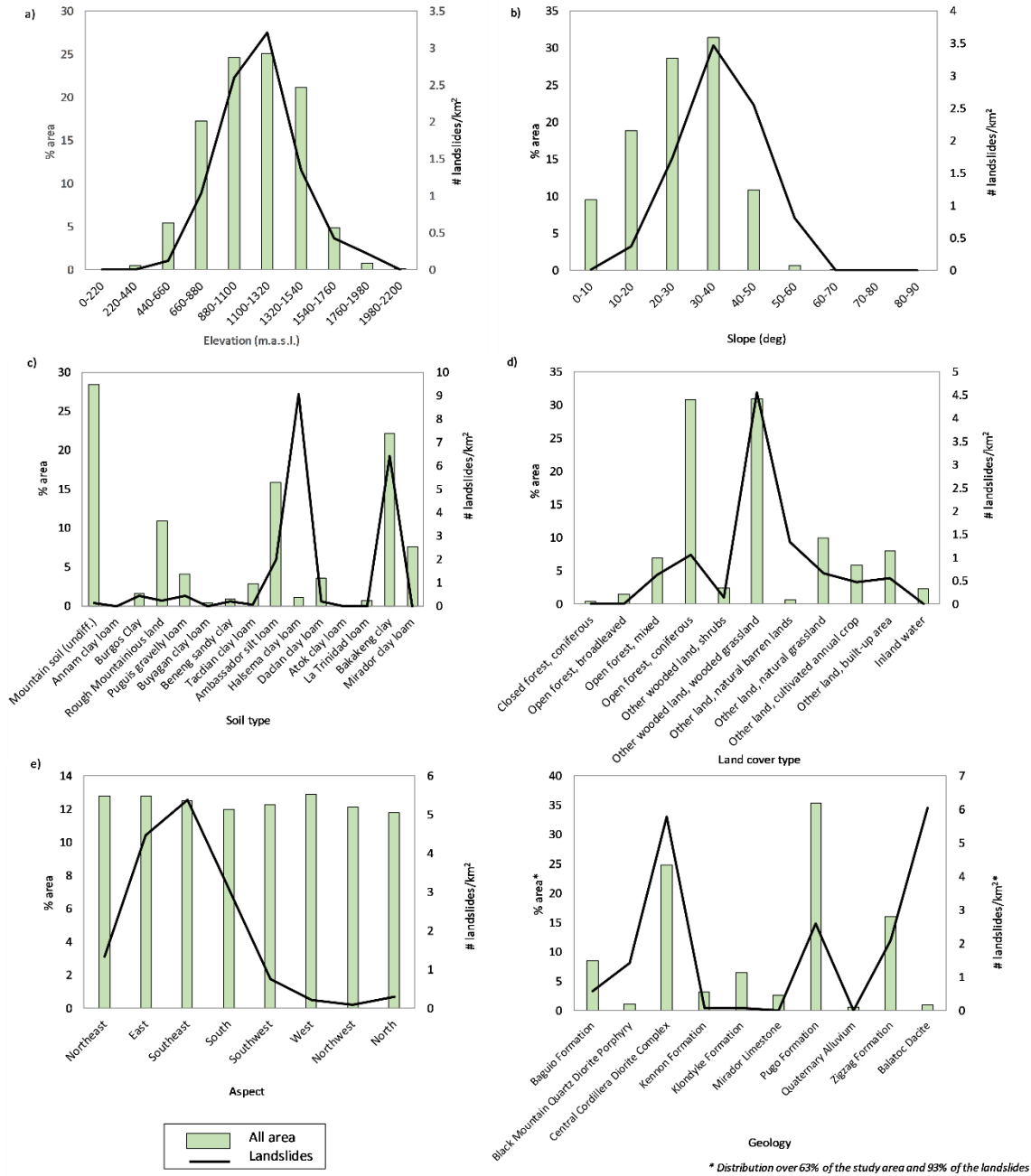


**Figure 2:** a) GPM IMERG data showing the evolution of Typhoon Mangkhut over the Philippines on the between 13 and 15 September 2018; b) Accumulated rainfall during Typhoon Mangkhut (13/09/2018 19:30 to 15/09/2018 15:30 UTC) within the study area and its surroundings, according GPM IMERG data (map) and rain gauge records in Baguio city (black triangle).



665

**Figure 3: Exceedence probability distribution for the 1101 landslide areas in the inventory, fit with theoretical power law model by the maximum likelihood method.**



670

**Figure 4: Histograms of different geomorphological parameters over the study area and frequency of landslides for every parameter class. The geomorphological parameters are: a) Elevation, b) Slope; c) Soil type; d) Land cover type; e) Aspect; f) Geology. Note that Geology is only over the 63% of the study area and 93% of the landslides as the Geology Map was only available for part of the area.**

675



a)



b)



c)

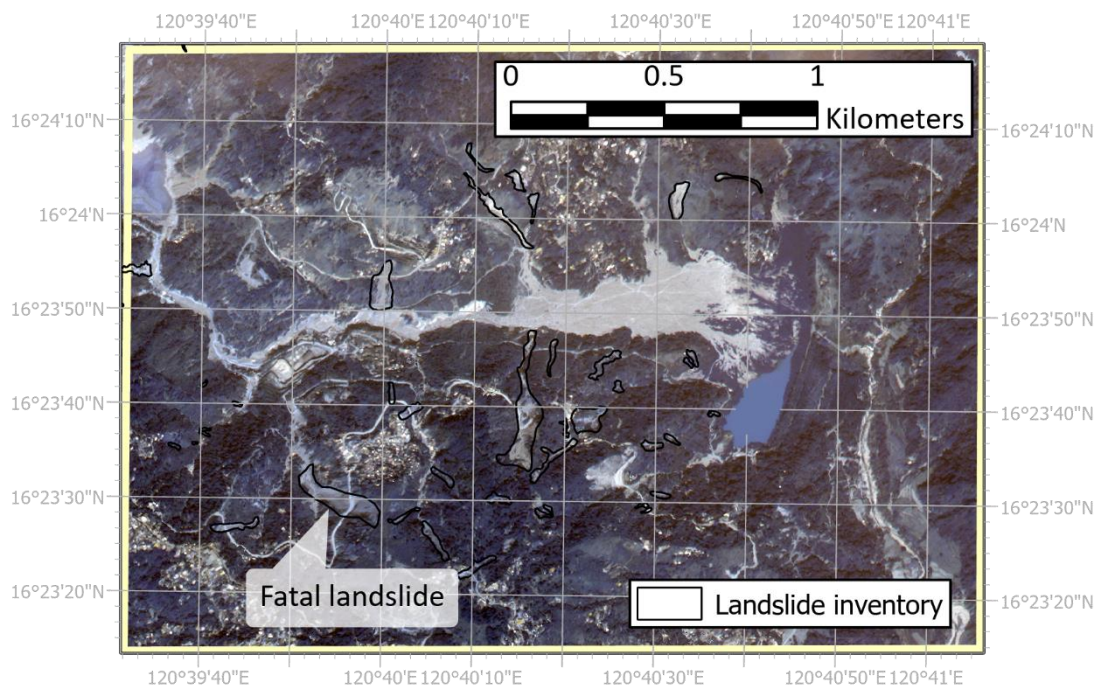
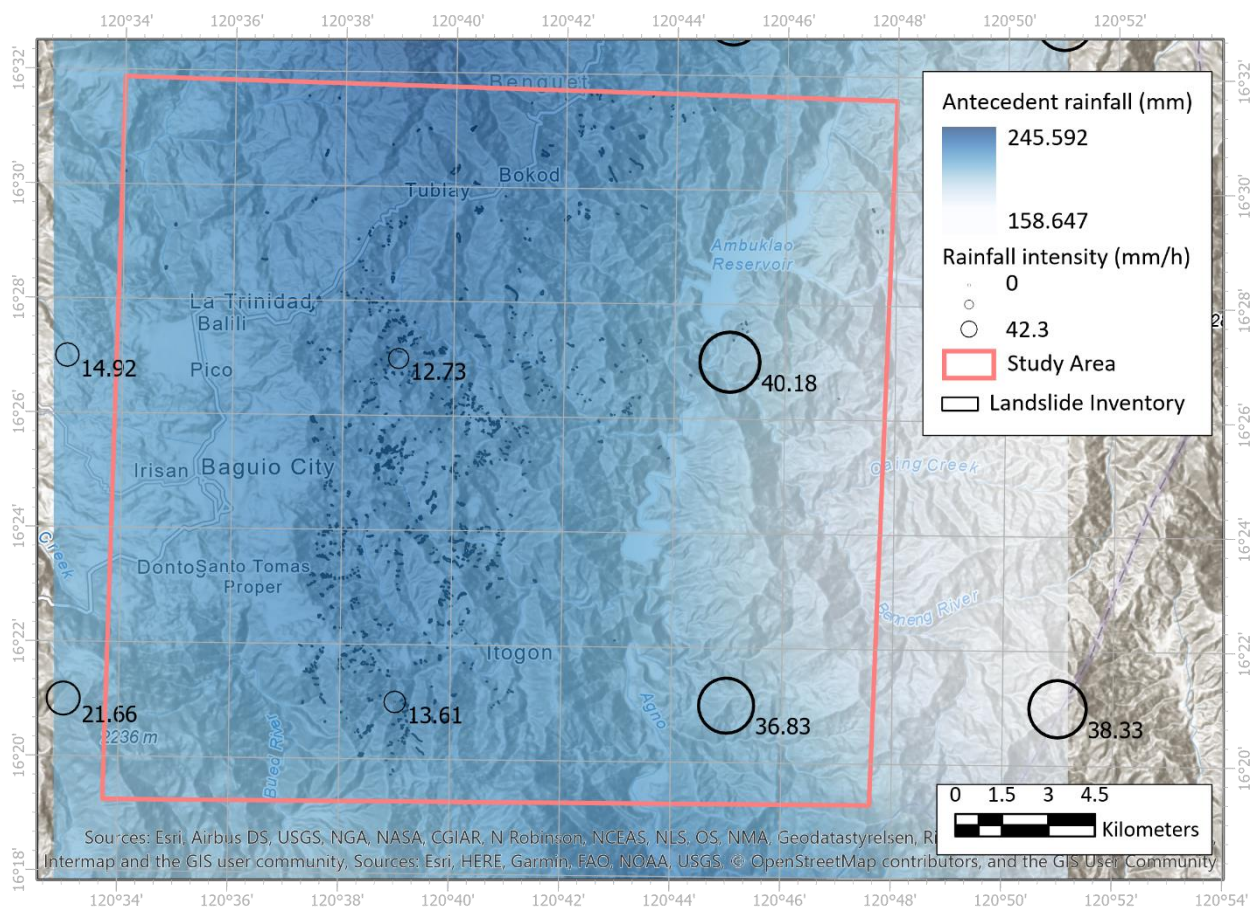
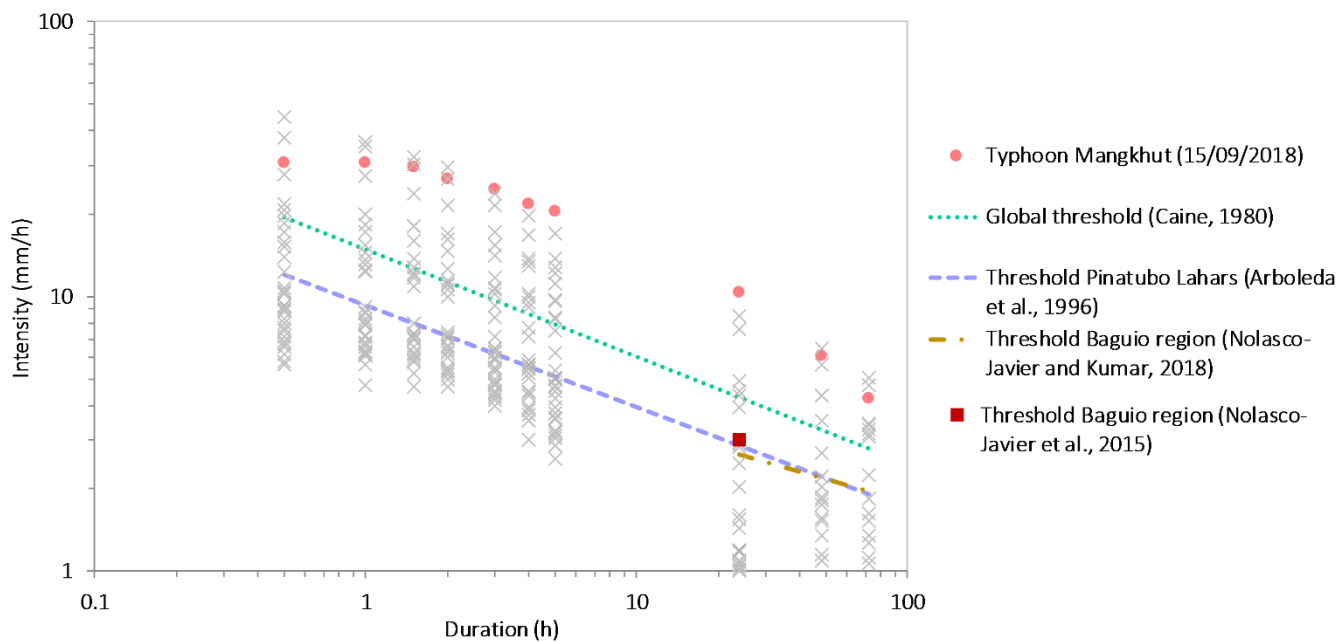


**Figure 5:** a) General view of the initiation area of the fatal landslide in Barangay Ucab that killed more than 80 miners; b) view of the particularly long runout of the landslide, from the road facing downhill and c) location of the landslide (see yellow rectangle in Figure 1 for the exact location within the study area). Satellite imagery from Worldview (02/03/2019).



685 **Figure 6: Colour gradient represents the antecedent rainfall, accumulated during the 13 days before the Typhoon. The values in the GPM IMERG grid points indicate the rainfall intensity on the 15 September 2018 at 03:30 UTC (maximum intensity in the study area)**

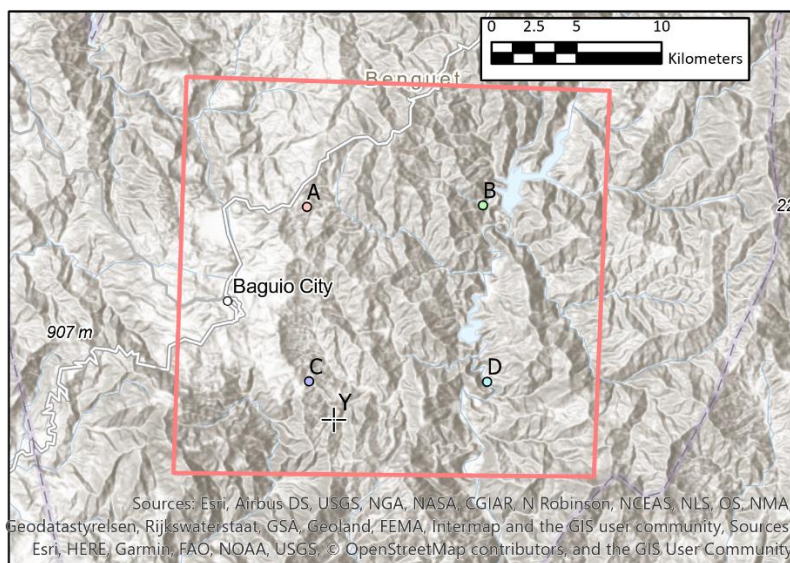


690

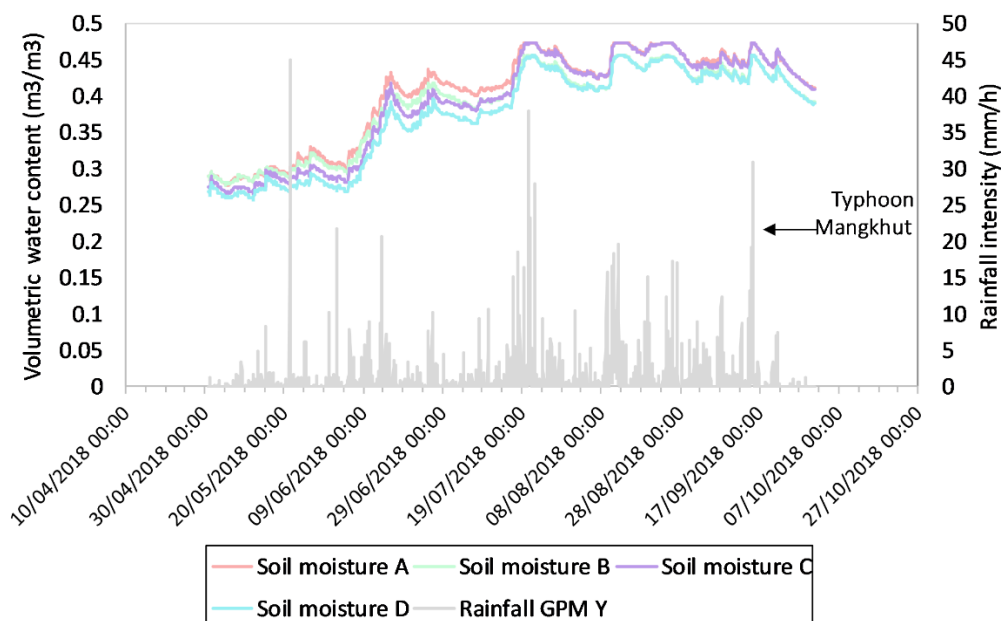
**Figure 7: Intensity-Duration correlations of rainfall associated to Typhoon Mangkhut as well as 33 high intensity rainfalls along 2018 in the study area. The rainfalls are compared to some global and regional thresholds published in the literature.**



a)

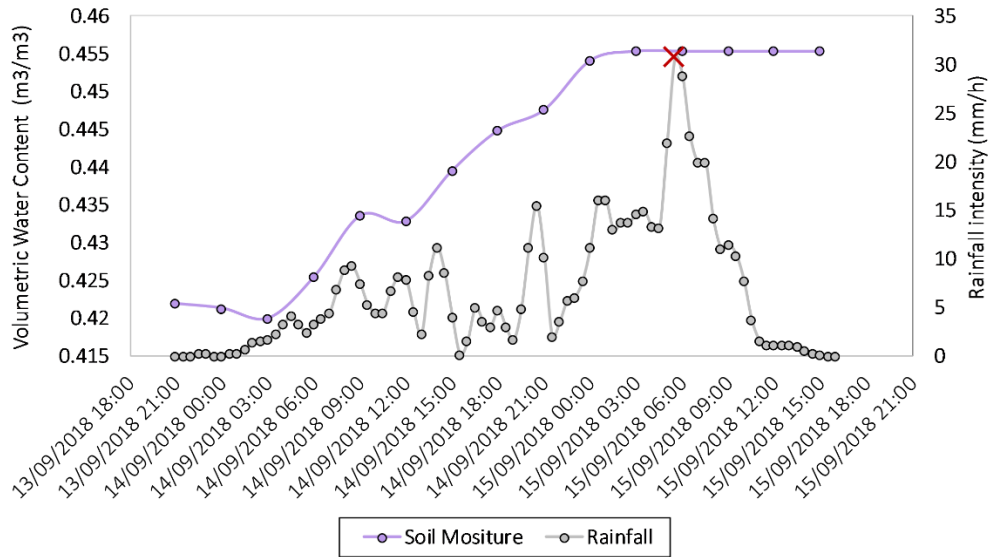


b)



695

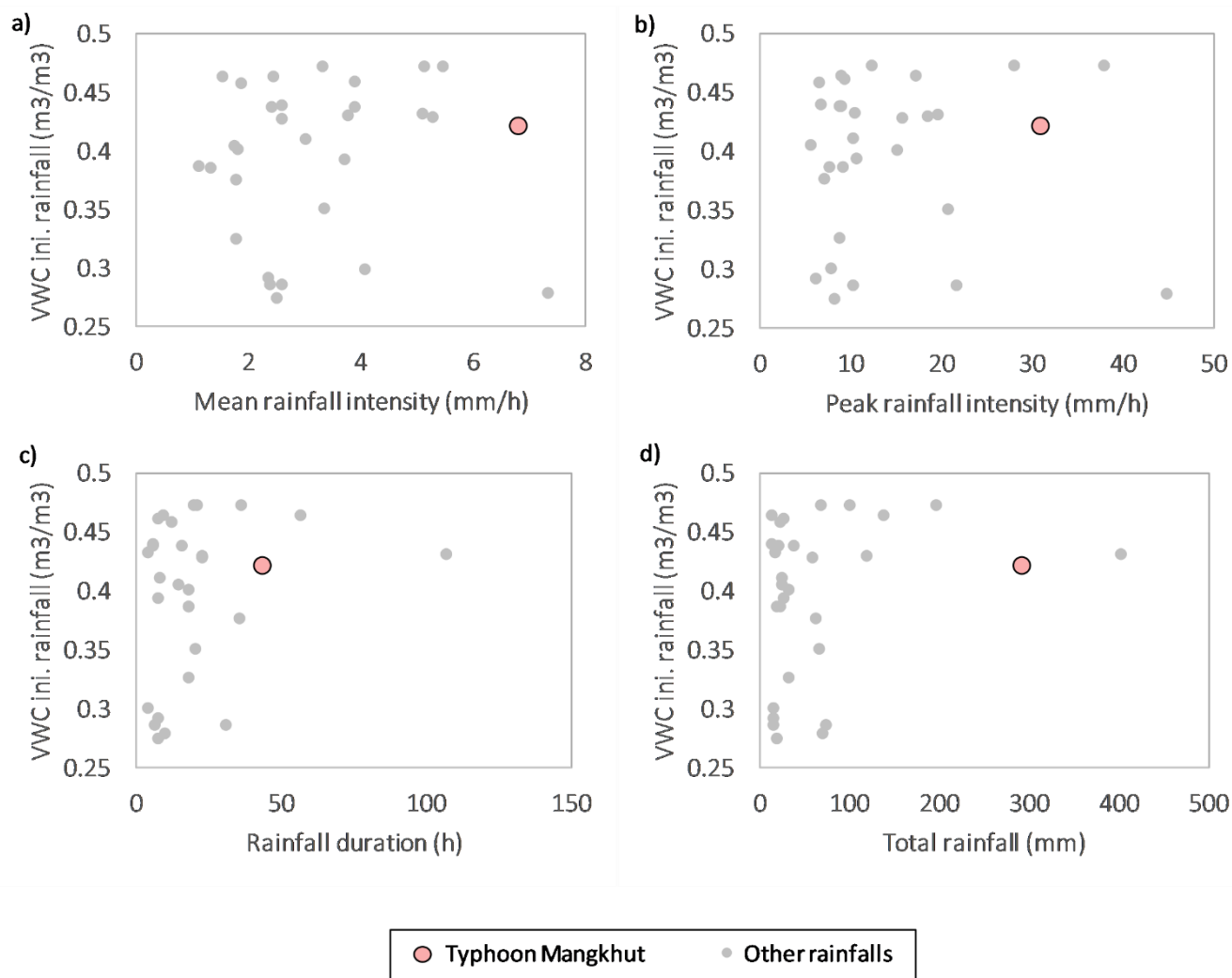
**Figure 8:** a) Location of SMAP-L4 and GPM IMERG grid points from which the soil moisture and rainfall data has been obtained within the study area and b) evolution of soil moisture (in volumetric water content) in A to D and rainfall in Y from the beginning of May to the end of September 2018.



700

**Figure 9: Detail of rainfall (GPM IMERG) and soil moisture (SMAP-L4) in points Y and C (see Figure 8a) respectively, during Typhoon Mangkhut. The red cross indicates the estimated time of the landslide occurrence (in UTC).**

705



710

**Figure 10: Correlation between soil moisture a) mean rainfall intensity of the event (total rainfall/rainfall duration), b) peak rainfall intensity during event, c) duration of the rainfall and d) accumulated rainfall during the event for the 33 (and Typhoon Mangkhut) high intensity rainfalls in the study area (see Figure 7). Soil moisture data obtained from SMAP-L4 data at point C and rainfall data from GPM IMERG at point Y (see Figure 8).**

715